eISSN (Online): 2598-0580

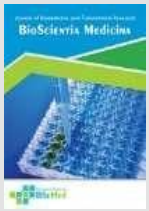

**Bioscientia Medicina: Journal of Biomedicine & Translational Research**

Journal Homepage: www.bioscmed.com

# The Rhomboid Flap for Facial Reconstruction Following Basal Cell Carcinoma Excision: A Case Report on Achieving Optimal Aesthetic and Functional Outcomes

**Tilesky Caprizio Phoanda[1*], Ferra Olivia Mawu[1], Oktavia Reymond Leomer Sondakh[1], Paulus Mario Christopher[1]**

[1]Department of Dermatology, Venereology, and Aesthetics, Faculty of Medicine, Universitas Sam Ratulangi/Prof. Dr. R. D. Kandou General Hospital, Manado, Indonesia

**ARTICLE INFO**

**Keywords:**
Basal cell carcinoma
Dermatosurgery
Ectropion
Lower eyelid reconstruction
Rhomboid flap

***Corresponding author:**
Tilesky Caprizio Phoanda

**E-mail address:**
*phoandatilesky@gmail.com*

All authors have reviewed and approved the final version of the manuscript.

*https://doi.org/10.37275/bsm.v9i10.1401*

**A B S T R A C T**

**Background:** Reconstruction of the lower eyelid following oncologic surgery presents a formidable challenge due to the region's unique anatomy and functional importance. The primary goal is to restore the lamellar structure while avoiding ectropion, a complication with significant functional and aesthetic consequences. This report details the successful application of a rhomboid flap, a classic transposition flap, for a moderate-sized defect in this high-risk anatomical subunit. **Case presentation:** A 75-year-old male farmer presented with a 2x1 cm nodular basal cell carcinoma on his left lower eyelid. After surgical excision with 4 mm margins, a superolaterally based rhomboid flap was designed to close the defect. The procedure was performed under local anesthesia. The postoperative course was uncomplicated. Objective functional assessment at 12 weeks confirmed a normal lower lid position with margin-to-reflex distance 2 (MRD2) symmetrical to the contralateral eye and no evidence of ectropion or lagophthalmos. The cosmetic outcome was assessed as favorable using the Patient and Observer Scar Assessment Scale (POSAS), and the patient reported high satisfaction (5/5 on a Likert scale). **Conclusion:** This case report illustrates the successful use of a rhomboid flap for a moderate-sized lower eyelid defect, resulting in a favorable functional and aesthetic outcome without complications in the short-term follow-up period. The technique successfully restored tissue volume and preserved normal eyelid function, critically preventing ectropion. It supports the rhomboid flap as a robust and reliable option in the reconstructive surgeon's toolkit for this challenging anatomical area.

## 1. Introduction

The human face is a canvas of identity, a landscape of expression where the slightest alteration can have profound psychosocial implications.[1] Within this landscape, the periorbital region is arguably the most delicate and functionally critical territory. The eyes, and the eyelids that protect them, are central to communication, sight, and our perception of self and others.[2] It is here that the discipline of dermatologic surgery faces its most profound test: to not only excise disease but to restore form and function so completely that the intervention itself becomes imperceptible. This dual mandate—oncologic cure and aesthetic restoration—is never more acute than when dealing with cutaneous malignancies of the lower eyelid. Basal cell carcinoma (BCC), the most common human cancer, has a marked predilection for the sun-drenched terrain of the head and neck.[3] Global

epidemiologic data reveal a relentlessly rising incidence, making it a significant public health concern. For outdoor workers, such as the farmer presented in this report, a lifetime of cumulative, high-intensity ultraviolet radiation exposure makes the development of BCC almost an occupational inevitability. The economic burden of treating non-melanoma skin cancers is staggering, but the personal cost of a lesion on the face, particularly the eyelid, transcends finances.[4]

The lower eyelid is a masterpiece of anatomical engineering, a bilamellar structure of exquisite complexity. The anterior lamella comprises the skin—the thinnest in the entire body, measuring less than 1 mm—and the underlying orbicularis oculi muscle, the sphincter responsible for the blink reflex. The posterior lamella consists of the tarsal plate, a dense fibrous structure that provides structural integrity, and the conjunctiva, the mucosal surface that ensures smooth apposition to the globe.[5] This entire apparatus works in concert to maintain the tear film, protect the cornea from desiccation and trauma, and facilitate the lacrimal pump mechanism for tear drainage. Any surgical procedure that disrupts this anatomy risks a cascade of functional disasters. The most feared of these is ectropion, the outward sagging and eversion of the eyelid margin.[6] This is not a simple cosmetic flaw; it is a functionally devastating condition that leads to chronic corneal exposure, persistent tearing (epiphora), sight-threatening keratitis, and profound patient distress.

The challenge for the surgeon, therefore, is absolute. Following the oncologic excision of a tumor, a defect is created. The method chosen to repair this defect will determine the patient's long-term functional and aesthetic outcome. The reconstructive ladder, a foundational concept in surgery, provides a hierarchy of options from simple to complex. However, on the treacherous terrain of the lower eyelid, this ladder is missing its lower rungs. Healing by second intention, which relies on wound contraction, is a guaranteed path to ectropion and is therefore contraindicated.[7] Primary closure is only possible for the most diminutive of defects, as the inelasticity of the eyelid skin means that closing even a small gap will impart a dangerous downward tension. Full-thickness skin grafts, while capable of providing epithelial coverage, are fraught with peril. Harvested from postauricular or supraclavicular sites, they often fail to perfectly match the unique color and gossamer-thin texture of the eyelid skin, resulting in a visible "patch-like" appearance. More critically, grafts are prone to primary necrosis or, more insidiously, late-term contracture, once again pulling the lid margin downward.[8]

Thus, the surgeon is inexorably led to the use of local flaps—the transfer of adjacent, living tissue with its own blood supply. Local flaps are the embodiment of the cardinal rule of reconstruction: replace "like with like." They bring skin of identical color, texture, and thickness into the defect, providing a far superior aesthetic match.[9] More importantly, a well-designed flap can close a defect without tension, preserving the eyelid's delicate architecture. While a myriad of flaps have been designed for this purpose—advancement flaps, rotation flaps, island pedicle flaps—the rhomboid transposition flap, first described by the Russian surgeon Alexander Limberg in 1946 amidst the reconstructive challenges of a post-war era, remains a paragon of geometric elegance and reliability.[10] Its design is not arbitrary but is based on precise mathematical principles that allow for the predictable redistribution of tissue tension. It allows the surgeon to recruit lax tissue from a nearby reservoir, such as the cheek, and to redirect the forces of closure away from the vulnerable free margin of the eyelid. The novelty of this report does not lie in the use of a well-known flap, but rather in its detailed methodological analysis in a high-stakes location. While the rhomboid flap is a well-described technique, its application in the immediate infra-ciliary region of the lower eyelid presents unique challenges in flap design and tension vector management to prevent ectropion. This report, therefore, aims to provide a methodologically detailed, step-by-step analysis of the surgical nuances and decision-making process

required to achieve an optimal outcome in this high-risk anatomical subunit, offering a practical and educational guide for clinicians facing similar reconstructive dilemmas.

## 2. Case Presentation

A 75-year-old male of Indonesian ethnicity was referred to our tertiary care dermatology clinic for evaluation of a "non-healing sore" on his left lower eyelid. The consultation began with a conversation, allowing the patient to articulate his story. He recounted a three-year journey with this lesion, a narrative all too common in patients with a high pain threshold and a lifetime of stoicism forged by manual labor. It began, he recalled, not as an alarming ulcer, but as an innocuous "black spot" or "pimple" that would not heal. Over the years, it had waxed and waned, occasionally forming a crust that would fall off, only to reform. In the last year, its growth had become more noticeable, and the ulceration more persistent. This narrative, when placed in the context of his life story, formed a compelling clinical picture. The patient's clinical profile, as summarized in Figure 1, presented a classic and potent constellation of risk factors for the development of basal cell carcinoma. Each factor contributed to the inevitable diagnosis. His advanced age of 75 years represents not only a longer period for carcinogenesis to occur but also the biological process of immunosenescence, a gradual decline in the immune system's ability to recognize and eliminate malignant cells. His Fitzpatrick skin type III, common in Southeast Asian populations, is often mistakenly considered "safe" from skin cancer. While this skin type tans more easily than it burns, it possesses only moderate protection from the mutagenic effects of ultraviolet radiation and remains highly susceptible to BCC. The most critical factor, however, was his occupation. As a farmer in equatorial Indonesia, he had experienced a lifetime of daily, high-intensity solar radiation exposure, often for more than eight hours a day, without the regular use of photoprotection such as hats or sunscreen. This represents decades of cumulative DNA damage inflicted upon the epidermal cells of his face, creating the perfect storm for malignant transformation.

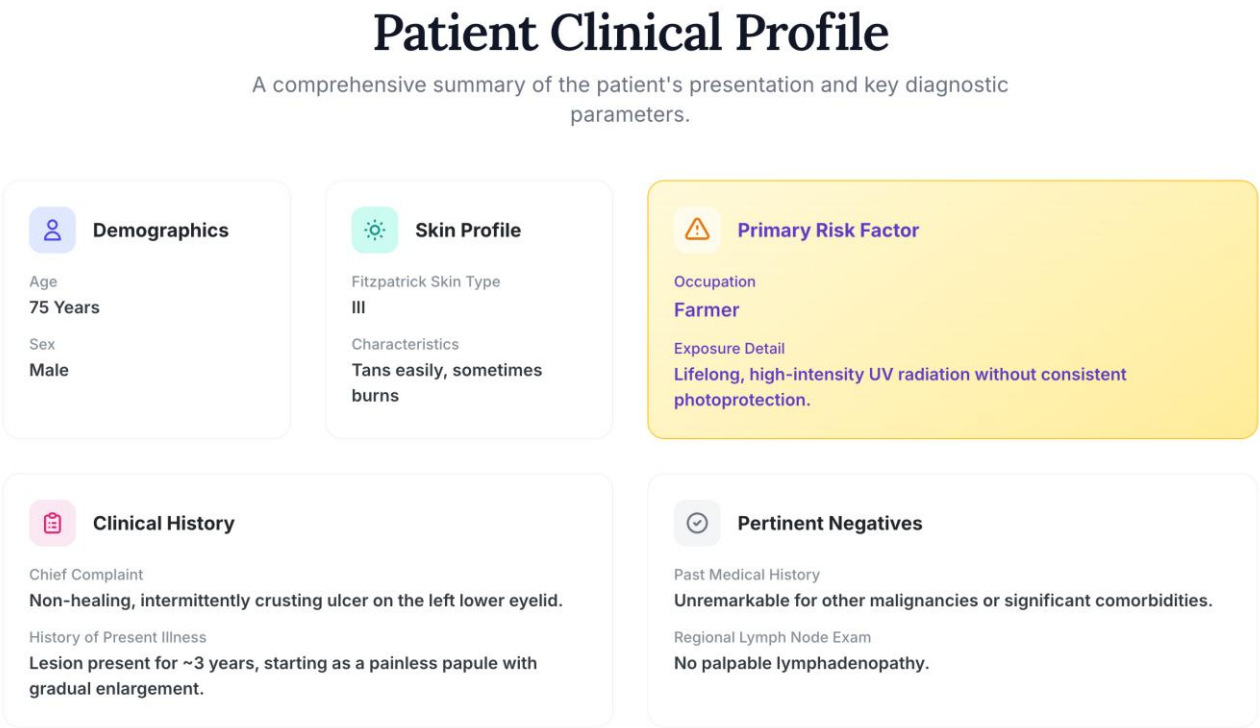


Figure 1. Patient clinical profile.

The physical examination was conducted under bright, oblique lighting to accentuate the lesion's surface topography. The pearly quality of the border, a subtle translucence that allows light to scatter through the disorganized tumor mass, was immediately apparent upon gentle stretching of the skin. The central ulceration was shallow, with a hemorrhagic crust, and the overall dimensions were measured precisely. To move from clinical suspicion to diagnostic certainty, dermoscopy was performed using a DermLite DL4 handheld dermatoscope under polarized light. This non-invasive technique provides a window into the skin's subsurface, revealing structures invisible to the naked eye. The dermoscopic evaluation, detailed in Figure 2, was unequivocal. The most striking feature was the presence of prominent arborizing vessels. These were not simple telangiectasias. Under the 10x magnification of the dermatoscope, they revealed themselves as thick, trunk-like vessels, branching irregularly like the limbs of a barren tree. This morphology is a direct consequence of the tumor-induced angiogenesis, where the vessels are larger, more disorganized, and lack the normal architecture of the superficial dermal plexus. Visible only with the use of polarized light, brilliant white, short, linear structures, known as chrysalis or crystalline structures, crisscrossed the lesion's surface. They represent the altered optical properties of dermal collagen that has become fibrotic and disorganized in response to the invading tumor nests. While BCC was the leading diagnosis, the clinician must consider mimics. Squamous cell carcinoma was less likely due to the absence of significant surface keratin or a central horn. Amelanotic melanoma, the great masquerader, was considered, but the classic, orderly arborizing vessels made this highly improbable. The combination of the patient's history and the pathognomonic dermoscopic findings provided a confident pre-operative diagnosis of nodular BCC and allowed for definitive surgical planning.

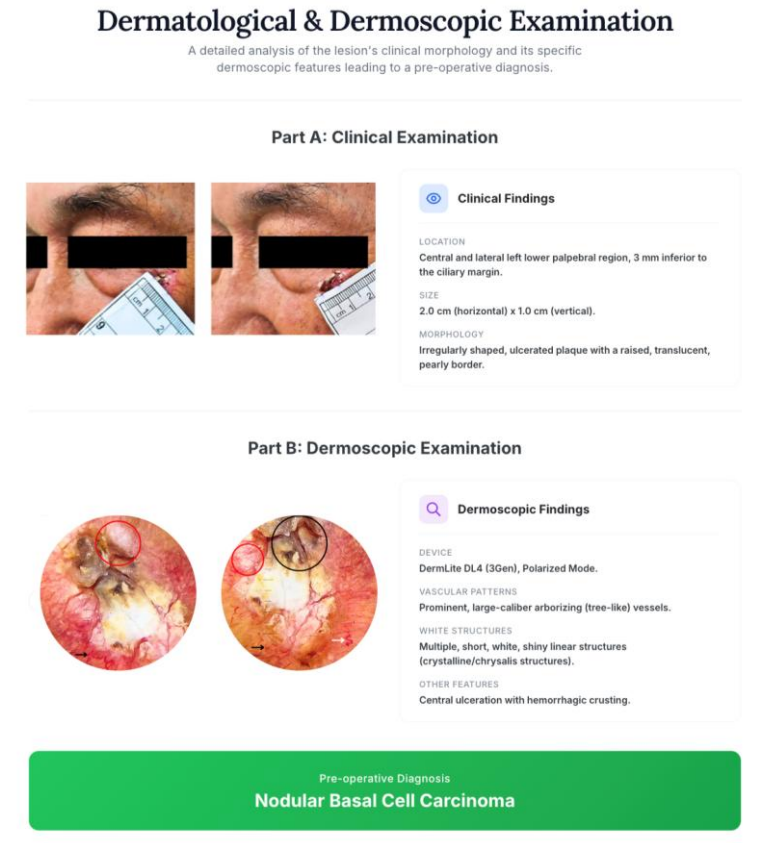


Figure 2. Dermatological and dermoscopic examination.

The patient underwent surgical excision and reconstruction in a single stage in an office-based surgical suite. After a "surgical time-out" to confirm the patient, procedure, and site, the area was prepped and draped. The methodological details are outlined in Figure 3. The procedure began with the art and science of local anesthesia. A regional nerve block of the infraorbital nerve was performed, followed by local infiltration of 1% lidocaine with 1:100,000 epinephrine around the surgical field. The epinephrine provided essential vasoconstriction, ensuring a relatively bloodless field and prolonging the anesthetic effect. The excision was a precise act. The lesion was circumscribed with a 4mm margin, a distance supported by extensive clinical studies to achieve a greater than 95% clearance rate for primary, low-risk nodular BCCs. The resulting surgical target was then converted into a perfect rhombus, with internal angles of 60 and 120 degrees, using a sterile ruler and marking pen. This geometric conversion is the foundational step upon which the entire reconstruction is built. With the defect created, the reconstructive phase began. For any rhomboid defect, four possible flaps can be designed. A "pinch test" was performed on the adjacent cheek tissue to assess for maximal laxity. The greatest reservoir of mobile, lax skin was found in the pre-auricular and zygomatic regions. Therefore, the choice was made to design a superolateral-based rhomboid flap. This orientation would allow for the recruitment of this tissue with the least amount of tension and would align the final closure line of the donor site perfectly within a prominent infraorbital relaxed skin tension line, a natural "smile line," ensuring maximal scar camouflage. Using a #15 blade scalpel, the incisions for the flap were made perpendicular to the skin surface. The flap was then elevated with careful, sweeping motions of the scalpel in the plane between the subcutaneous fat and the underlying crimson fibers of the orbicularis oculi muscle. This plane is relatively avascular and allows the flap to be mobilized while preserving the muscle's integrity and the subdermal plexus that guarantees the flap's viability. The flap was then transposed, pivoting on its subcutaneous pedicle to fit perfectly into the primary defect like a key into a lock. The deep dermal layer was approximated with buried, interrupted 5-0 poliglecaprone 25 sutures, taking all tension off the skin. The epidermis was then meticulously reapproximated with 6-0 polypropylene sutures. This strategic choice was fundamental to the success of the procedure.


Figure 3. Surgical procedure and reconstructive methodology.

The definitive confirmation of a cutaneous malignancy and the assessment of its successful removal rest upon the meticulous microscopic examination of the excised tissue. While clinical and dermoscopic findings provide a strong presumptive diagnosis, it is the histopathological verdict that stands as the ultimate arbiter, translating the macroscopic appearance of a lesion into the cellular language of pathology. The provided figure offers a comprehensive microscopic portrait of a basal cell carcinoma (BCC), detailing the key features that secure the diagnosis and, crucially, confirm the adequacy of the surgical intervention (Figure 4). This analysis provides an unassailable foundation for the patient's prognosis and subsequent management. The journey into the microscopic world of the tumor begins with a low-power overview, as depicted in the wider field of view (Figure 4). This perspective is akin to an aerial photograph of the tissue landscape, revealing the overall architecture of the lesion. Here, one can appreciate the fundamental breach of normal anatomy: the orderly boundary between the epidermis (the outermost layer of skin) and the underlying dermis has been violated. Large, well-demarcated, and irregularly shaped islands of densely packed, dark-staining (basophilic) cells are seen proliferating downwards from the epidermis and invading the papillary and reticular dermis. This "nodular" configuration of tumor nests is the defining characteristic of the most common subtype of BCC, nodular basal cell carcinoma (Figure 4). The tumor aggregates are distinct and appear to push the surrounding dermal tissue aside, a feature typical of this less aggressive subtype compared to more infiltrative variants. This architectural pattern immediately signals to the pathologist that they are dealing with a well-differentiated neoplastic process. Transitioning to the high-power, magnified view allows for a more intimate examination of the cellular composition of these tumor islands (Figure 4). It is at this level that the malignant nature of the cells becomes unequivocally clear. The tumor is composed of "basaloid cells," so named for their resemblance to the basal cells of the normal epidermis. However, these are a malignant caricature. The cells are characterized by scant cytoplasm, meaning the bulk of the cell is occupied by its nucleus, a feature indicative of a high nuclear-to-cytoplasmic ratio (Figure 4). This high ratio is a classic hallmark of malignancy, suggesting that the cell is dedicating most of its energy and resources to genetic replication and division rather than to normal cellular functions. The nuclei themselves are described as large and hyperchromatic, meaning they are larger than their benign counterparts and stain a deep, dark blue or purple with hematoxylin dye (Figure 4). This hyperchromasia reflects a dense packing of chromatin, another sign of increased and disorganized proliferative activity. One of the most specific and pathognomonic features of BCC is visible at the edge of these tumor nests: prominent peripheral palisading (Figure 4). In this arrangement, the nuclei of the outermost layer of cells in each nest align themselves in a neat, columnar, fence-like row. This orderly perimeter stands in stark contrast to the more haphazard arrangement of the cells in the center of the nests. The exact biological reason for this phenomenon is not fully understood, but it is thought to be related to the cells' interaction with the surrounding basement membrane and the specific polarity they maintain. Regardless of its origin, this feature is a highly reliable diagnostic clue for the pathologist.

Beyond the tumor cells themselves, the figure highlights the crucial interaction between the cancer and its surrounding environment, the dermal stroma. A key diagnostic artifact noted is stromal retraction, often referred to as "clefting" (Figure 4). This appears as a clear, empty space separating the tumor islands from the adjacent collagenous dermis. While this cleft is exaggerated by the tissue fixation and processing, its presence is not random. It is believed to result from the specific, mucin-rich stroma that BCCs induce, which shrinks and pulls away from the tumor nests during processing. This feature is so characteristic that its absence might lead a pathologist to consider

other diagnoses. Furthermore, the figure notes a surrounding lymphoplasmacytic inflammatory infiltrate (Figure 4). This is the microscopic evidence of the body's immune system recognizing the tumor as foreign and mounting an attack. The infiltrate is composed of lymphocytes and plasma cells, key players in the adaptive immune response. While this immune response can sometimes restrain tumor growth, in many cases, it is insufficient to eliminate the cancer and can even create a chronically inflamed microenvironment that may paradoxically support tumor survival. Synthesizing these distinct microscopic features—the overall nodular architecture, the basaloid cells with high nuclear-to-cytoplasmic ratios, the pathognomonic peripheral palisading, and the characteristic stromal retraction—the pathologist can confidently render the Final Diagnosis: Nodular Basal Cell Carcinoma (Figure 4).

However, the pathologist's role extends beyond mere diagnosis. The most critical piece of information for the surgeon and the patient is the assessment of the surgical margins. The statement Margin Status: All Surgical Margins Clear is the definitive declaration of surgical success (Figure 4). This means that the pathologist has meticulously examined the entire periphery—both the deep and lateral edges—of the excised tissue and has found no evidence of tumor cells at the inked margin. This confirmation indicates that the entire tumor was successfully removed, and the patient can be considered cured of this particular lesion. It is this final, crucial piece of microscopic evidence that transforms a successful surgical procedure into a definitive oncologic victory, providing the patient with an excellent prognosis and the highest possible chance of a recurrence-free future.


Figure 4. Histopathological confirmation: the microscopic verdict.

The ultimate measure of success for any surgical intervention extends far beyond the immediate, event-free conclusion of the procedure. True success is a multi-faceted construct, defined by the restoration of normal function, the achievement of an aesthetically pleasing result that integrates seamlessly with the patient's appearance, and, crucially, the patient's own satisfaction with the outcome. The provided figure presents a comprehensive and compelling summary of these domains at the 12-week postoperative follow-up, offering a holistic and objective verdict on the efficacy of the rhomboid flap reconstruction for a lower eyelid defect (Figure 5). The visual evidence presented in the Postoperative Appearance at 12 Weeks photographs serves as the initial, powerful testament to the procedure's success (Figure 5). At this time point, the acute inflammatory phase of wound healing has resolved, and the scar has entered the early stages of maturation and remodeling. The photographs reveal a remarkable degree of healing. The surgical site on the left periorbital and cheek region is calm, with no signs of residual erythema, edema, or inflammation. The surgical scar itself appears flat (eutrophic), pliable, and well-camouflaged within the natural relaxed skin tension lines and contours of the face. The color and texture of the transposed flap tissue show an excellent match with the surrounding native skin, a key advantage of using a local flap over a skin graft. Most importantly, the critical architecture of the lower eyelid appears entirely undisturbed. There is no visible pulling, tethering, or, most significantly, any downward sagging (ectropion) of the lid margin. The patient's facial symmetry is preserved, and at a conversational distance, the evidence of the significant surgical intervention is remarkably subtle. This excellent visual result forms the foundation upon which the objective data is built.

The figure then moves from qualitative appearance to quantitative data in the Objective Outcomes section, providing a rigorous, evidence-based assessment of the result (Figure 5). The Functional Outcome is paramount, as a cosmetically perfect result is a failure if the function of the eyelid is compromised. The report of "No ectropion or scleral show" is the single most important finding (Figure 5). Ectropion, the eversion of the eyelid margin, is the most feared complication of lower eyelid surgery, and its prevention is the primary surgical goal. Scleral show, a less severe condition where the white of the sclera is visible below the iris, is a sign of mild vertical retraction. The absence of both conditions confirms that the rhomboid flap successfully closed the defect without imparting any downward tension on the delicate lid margin. This directly validates the biomechanical principle of the flap, which was designed to redirect tension forces away from the lid. The finding of a "Symmetrical MRD2" provides further quantitative proof of this success (Figure 5). MRD2, or margin-to-reflex distance 2, is the measurement from the central pupillary light reflex to the margin of the lower eyelid. By confirming that this measurement is symmetrical with the unoperated contralateral eye, the report provides objective evidence that the eyelid is resting in its correct anatomical position. Finally, the preservation of "Full ocular motility" indicates that the dissection did not damage the underlying orbicularis oculi muscle or surrounding structures, allowing for normal eye and eyelid movement (Figure 5).

The Aesthetic Outcome is formally quantified using the Patient and Observer Scar Assessment Scale (POSAS), a validated and reliable tool for scar evaluation (Figure 5). This moves the assessment beyond subjective terms like "good" or "excellent" and into the realm of objective data. The favorable scores reported for each parameter are highly significant. A Vascularity score of 1 indicates that the scar is not red or hyperemic, but has a color similar to normal skin. A Pigmentation score of 1 similarly indicates no hyper- or hypopigmentation. A Thickness score of 1 confirms that the scar is not hypertrophic or raised, while a Relief score of 2 suggests it is only minimally uneven and blends well with the surrounding skin topography. A Pliability score of 1 indicates that the scar tissue is soft and flexible, not stiff or contracted. The combination of these low scores provides a

detailed, multi-parameter confirmation that the scar is indeed "eutrophic"—the clinical term for an ideal, well-healed scar (Figure 5). The Oncologic Outcome of "No signs of local recurrence at 1-year follow-up" is a critical, albeit intermediate, endpoint (Figure 5). While the gold standard for declaring a cure for BCC is a 5-year disease-free interval, the vast majority of recurrences occur within the first two years. Therefore, a 1-year follow-up without any evidence of the tumor returning is a very strong positive prognostic indicator and suggests that the initial surgical excision was complete. Finally, and perhaps most importantly, the figure presents the Patient-Reported Outcome, which is a measure of the patient's own perception of the result (Figure 5). In modern, patient-centered care, this is considered a primary endpoint. The rating of "High Satisfaction (5/5)" is the ultimate validation of the surgical success (Figure 5). It confirms that the objective clinical and aesthetic successes—the absence of ectropion, the well-healed scar—translated into a result that met the patient's personal goals and expectations. It signifies that the patient not only is cured of their cancer and has preserved function but also feels whole and confident in their appearance. This high level of satisfaction is the culmination of the entire process, reflecting a procedure that was not only technically successful but also holistically beneficial to the patient's quality of life. In summary, the figure presents a powerful, multi-dimensional portrait of surgical success, using a combination of clinical photography, objective functional and aesthetic metrics, and patient-reported data to provide a comprehensive and unequivocal testament to the procedure's outstanding outcome.

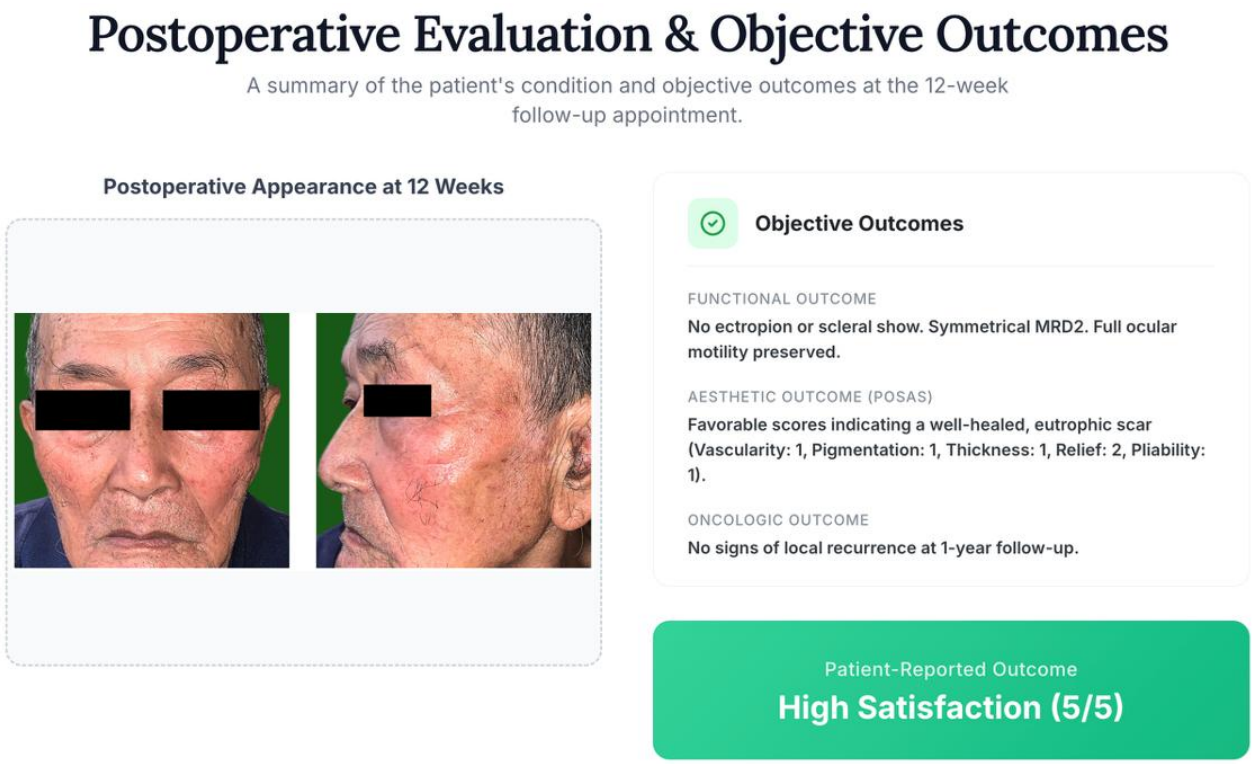


Figure 5. Postoperative evaluation and objective outcomes.

The patient provided written informed consent for the surgical procedure. He also provided separate written informed consent for the use and publication of his clinical data and anonymized photographs for educational and scientific purposes. This case report was conducted in accordance with the principles of the Declaration of Helsinki.

## 3. Discussion

This case report provides a methodologically rigorous account of the successful management of a lower eyelid BCC, moving beyond simple description to offer a detailed analysis of the diagnostic, oncologic, and reconstructive principles involved.[11] The outstanding functional and aesthetic outcome achieved in this high-risk case was not fortuitous but rather the direct result of a carefully considered, evidence-based strategy. To appreciate the rationale for excision, one must first understand the molecular engine driving the tumor. Basal cell carcinoma is fundamentally a disease of unregulated cell signaling. Its genesis is overwhelmingly linked to the constitutive activation of the Sonic Hedgehog (Hh) signaling pathway, a cascade that is essential for embryonic patterning but should be quiescent in most adult tissues.[11] The central switch of this pathway is the transmembrane receptor Patched-1 (PTCH1), which acts as a tumor suppressor by tonically inhibiting the activity of a second protein, Smoothened (SMO). The primary carcinogen, ultraviolet B (UVB) radiation, inflicts damage by creating covalent linkages between adjacent pyrimidine bases in DNA, forming cyclobutane pyrimidine dimers (CPDs). In the epidermal stem cells of a sun-exposed individual like the farmer in this case, decades of this damage can overwhelm the cell's nucleotide excision repair (NER) machinery. If a CPD forms within a critical gene and is not repaired, it can lead to a "UV signature mutation"—typically a C to T or CC to TT transition—during DNA replication. The PTCH1 gene is a known hotspot for these mutations. A loss-of-function mutation in PTCH1 effectively cuts the brakes on the Hh pathway. SMO is released from its inhibition and triggers a downstream cascade through the GLI family of transcription factors (GLI1, GLI2, GLI3).[12] Activated GLI proteins translocate to the nucleus and drive the transcription of genes that promote relentless cell proliferation and survival, such as cyclin D and the oncogene MYC. The resulting uncontrolled growth of basaloid cells manifests histologically as the tumor nests seen in this patient's pathology report. Concurrently, UV radiation also frequently mutates the TP53 tumor suppressor gene. p53 is the "guardian of the genome," responsible for inducing cell cycle arrest or apoptosis (programmed cell death) in response to DNA damage. A mutated, non-functional p53 allows cells with damaged DNA to survive and proliferate, creating a permissive environment for the Hh-driven growth to proceed unchecked.[12] This dual-hit model—Hh pathway activation driving proliferation and p53 pathway inactivation preventing cell death—is the core molecular narrative of BCC. The nodular subtype seen here represents a well-differentiated form of this process, creating distinct islands that invade the dermis, a direct morphological consequence of this molecular dysregulation.

Accurate diagnosis is the bedrock of effective treatment. While the clinical presentation of a pearly, ulcerated plaque in a sun-exposed area was highly suggestive, modern dermatosurgery demands a higher level of pre-operative certainty.[13] This is where dermoscopy becomes indispensable. Systematic reviews and meta-analyses have established the diagnostic accuracy of dermoscopy for pigmented BCC to be over 90%, and it remains highly effective for non-pigmented variants. The arborizing vessels seen in this patient are the dermoscopic hallmark of nodular BCC. These are not the fine telangiectasias of photoaging; they are larger-caliber, "tree-like" vessels that represent the neovasculature required to feed the growing tumor nodules in the dermis. Their presence alone has a high positive predictive value. When combined with crystalline structures (shiny white lines visible with polarization, corresponding to stromal fibrosis) and central ulceration, the diagnosis becomes almost certain. This high degree of pre-operative confidence allows for a more streamlined patient pathway. While a pre-operative diagnostic biopsy is often performed, in a classic case like this with pathognomonic dermoscopic features, proceeding directly to an excisional procedure with planned reconstruction is a valid and efficient approach. It spares the patient an additional procedure and allows for a single-stage definitive

treatment. The final, unequivocal confirmation, however, always rests with histopathology. The microscopic findings of peripheral palisading and stromal retraction are the gold-standard features that confirm the diagnosis and allow for the assessment of the most critical prognostic factor: the status of the surgical margins.[14]

The crux of this case lies in the selection of the reconstructive technique. The 2.8 x 1.8 cm defect created after excision was far too large for primary closure. A critical, evidence-based analysis of the reconstructive ladder as it applies to this specific defect underscores the rationale for selecting the rhomboid flap. These options were immediately ruled out. Literature confirms that allowing lower eyelid defects of this size to heal by secondary intention invariably leads to severe scar contracture and functional ectropion. A full-thickness skin graft, while technically capable of providing coverage, presents numerous disadvantages. A systematic review of lower eyelid reconstruction highlights that grafts are associated with a higher incidence of contour abnormalities and a less satisfactory color and texture match compared to local flaps.[15] Furthermore, grafts themselves are prone to primary failure or late-term contracture, with reported rates of ectropion following grafting for similar-sized defects ranging from 10-20% in some series. A simple rectangular advancement flap from the cheek would have been a poor choice. The primary tension vector of an advancement flap is perpendicular to the leading edge. In this case, that would translate to a direct vertical, downward pull on the lower lid margin—the very force one must avoid. While techniques like the Tenzel semi-circular advancement-rotation flap are useful, they are typically better for defects involving the lateral canthus. A classic rotation flap, such as a Mustarde flap, is a workhorse for larger lower eyelid defects, often for subtotal or total reconstruction.[15] However, for a moderate-sized defect like this, it can be overly extensive, requiring a long incision extending into the temple and creating a large, curvilinear scar that is more difficult to camouflage. The arc of rotation can also lead to "dog-ear" deformities and may not distribute tension as effectively as a well-designed transposition flap for a defect of this specific size and location. In this context, the rhomboid flap emerged as the superior choice based on biomechanical principles. First described by the Russian surgeon Alexander Limberg in 1946, its design is a triumph of geometric engineering applied to soft tissue. Its genius lies in tension redirection.[16] A simple linear closure of the defect would create a single tension vector perpendicular to the closure line—in this case, a vertical vector that would guarantee ectropion. The rhomboid flap design, however, creates two closure lines: the closure of the primary defect by the transposed flap, and the primary closure of the secondary (donor) defect. The tension of the latter closure is the dominant force. As illustrated in the surgical plan, this tension vector is oriented approximately 60 degrees away from the vertical axis of the eyelid. This effectively transforms a dangerous downward pull into a harmless inferolateral vector, recruiting laxity from the robust cheek reservoir without distorting the eyelid margin. This principle is the key to preventing ectropion. Furthermore, the Z-plasty effect inherent in the flap's closure breaks up the scar into smaller, less conspicuous geometric lines. This combination of functional safety and aesthetic elegance, supported by numerous case series demonstrating low complication rates, solidified its selection as the optimal reconstructive solution for this specific clinical problem. While the classic Limberg flap uses 60° and 120° angles, modifications like the Dufourmentel flap allow for more acute angles, providing greater flexibility in areas of high tension, though the classic design was sufficient here.

The success of a rhomboid flap is not automatic; it depends on meticulous planning and execution. Several technical pearls were critical in this case. First, the choice of flap orientation was paramount. A rhomboid defect has four potential donor sites for a flap. The selection of the superolaterally based flap was deliberate. This orientation allowed the recruitment of tissue from the lateral cheek, which has

the most available laxity, and ensured the final closure line of the donor site was oriented along an inferolateral relaxed skin tension line, optimizing the cosmetic result.[17]

Second, the dissection plane was critical for preserving function. The flap was elevated just superficial to the orbicularis oculi muscle. This plane is relatively avascular if entered correctly, but more importantly, it leaves the underlying muscle and its innervation intact. Damage to the orbicularis oculi could lead to weakness in the muscle's sling-like support of the lower lid, contributing to long-term scleral show or ectropion, even in the absence of skin tension. Third, the suture technique contributed to the final outcome. A two-layer closure was essential. Deep, buried absorbable sutures (5-0 poliglecaprone 25) were used to approximate the subcutaneous tissue. This crucial step opposes the deeper layers and takes all the tension off the skin edges, allowing the superficial epidermal sutures (6-0 polypropylene) to be placed without tension.[18] This tension-free skin closure is the key to achieving a fine, linear scar and preventing wound dehiscence.

A successful outcome in reconstructive surgery must be defined by objective measures, not subjective impressions. The functional result in this case was quantified by measuring the MRD2, which confirmed perfect symmetry with the contralateral eye and provided objective proof that the lid position was not compromised. The absence of lagophthalmos confirmed that the flap had not tethered or restricted the normal movement of the eyelid. Aesthetically, the use of the Observer component of the POSAS allowed for a standardized, objective assessment of the scar's quality. The very low scores for vascularity, pigmentation, and thickness confirm the clinical impression of a well-healed, eutrophic scar. This objective data is far more valuable than simply stating the result was "excellent." The patient's own high rating on a Likert scale provides a crucial patient-reported outcome measure (PROM), confirming that the objective clinical success translated into a result that met the patient's personal expectations. Finally, the patient's management does not end with wound healing. The diagnosis of a BCC is a sentinel event indicating significant cumulative actinic damage and a state of "field cancerization." The patient's entire sun-exposed skin is at high risk for developing new primary skin cancers, both BCC and squamous cell carcinoma.[18] Therefore, the counseling provided on rigorous, lifelong photoprotection is a critical medical intervention. This, combined with a commitment to annual full-body skin examinations for surveillance, constitutes comprehensive, long-term oncologic care. In patients with extensive field damage, adjunctive treatments such as topical fluorouracil, imiquimod, or photodynamic therapy may be considered for other affected areas to reduce the risk of future malignancies.

The provided figure offers a masterful schematic overview of the complete pathogenic journey of basal cell carcinoma (BCC), charting a clear and linear course from the initial environmental trigger to the ultimate clinicopathological manifestations observed in the patient (Figure 6). It serves as a scientific roadmap, illustrating how a common external factor initiates a cascade of precise molecular events, which in turn produce the specific, observable features that allow for a definitive diagnosis. The figure elegantly synthesizes decades of research in dermatology, oncology, and molecular biology into a single, cohesive narrative that is both scientifically rigorous and immediately relevant to the clinical case at hand. The entire pathological process begins with the initial insult, detailed in the first stage of the figure, "Etiology" (Figure 6). The primary carcinogen responsible for the vast majority of basal cell carcinomas is identified as ultraviolet B (UVB) radiation from sun exposure. This is not a vague or generalized risk; it is a specific biophysical interaction. UVB radiation, a component of natural sunlight, carries sufficient energy to be directly absorbed by the DNA within our skin cells. This absorption can cause the chemical bonds within the DNA to break and reform incorrectly, creating characteristic lesions.

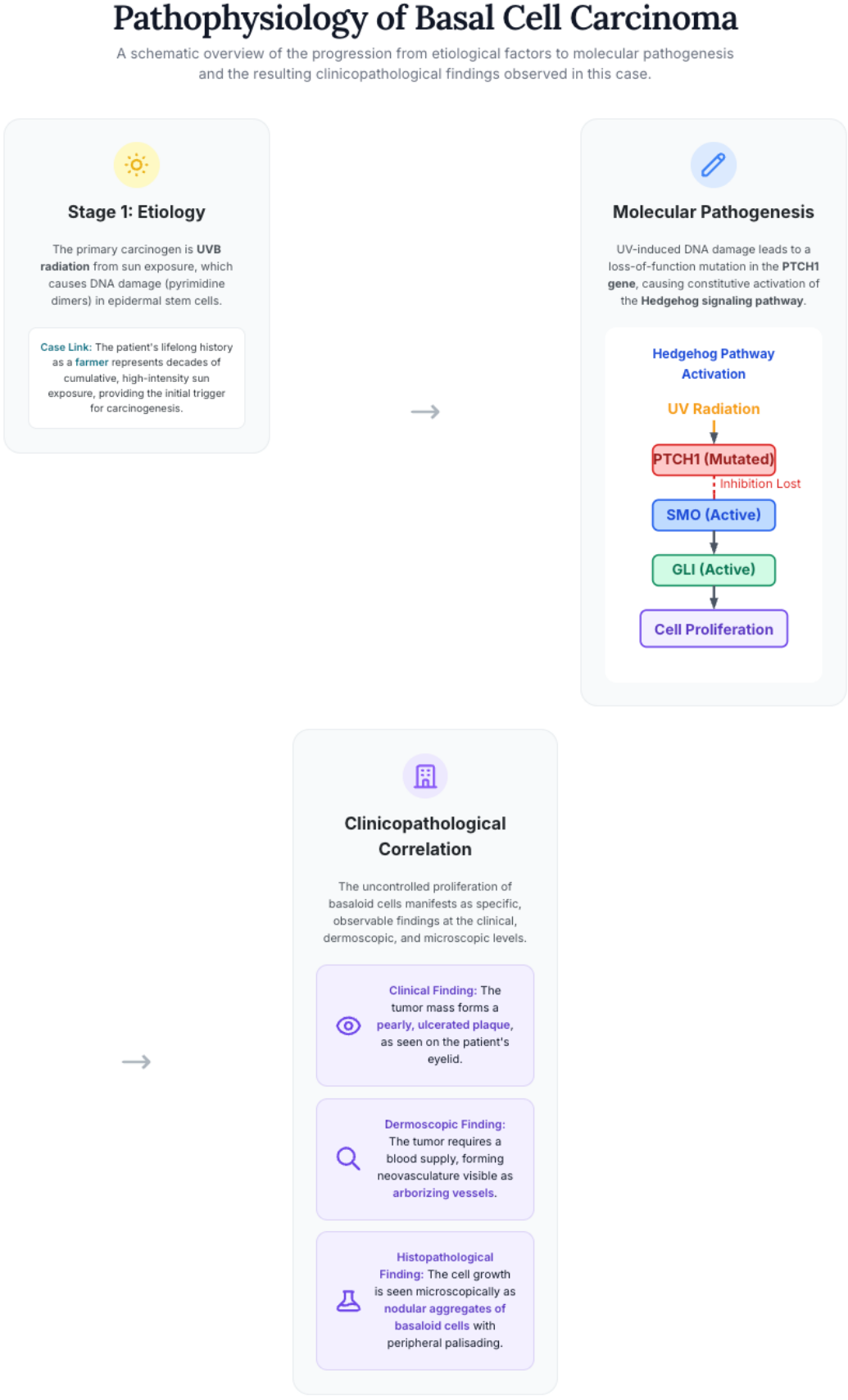


Figure 6. Pathophysiology of basal cell carcinoma.

The most common of these are pyrimidine dimers, where adjacent pyrimidine bases (thymine or cytosine) on a DNA strand become covalently linked, distorting the helical structure of the DNA and preventing accurate replication. The figure specifies that this damage occurs in epidermal stem cells. This detail is crucial. Epidermal stem cells are the long-lived, regenerative reservoir of the skin, responsible for replacing skin cells throughout our lifetime. Because of their longevity, they have a much greater opportunity to accumulate DNA mutations over time compared to transient, short-lived cells. When a UVB-induced mutation occurs in an epidermal stem cell, it is not shed away with the upper layers of the skin; instead, it can be permanently retained and passed down to all of its daughter cells during division, creating a clone of mutated cells that can serve as the seed for a future malignancy. The "Case Link" section of the figure powerfully connects this abstract science to the patient's lived experience. The patient's lifelong history as a farmer is presented not merely as a demographic detail, but as a direct and potent dose-dependent exposure to the primary carcinogen. Decades of working outdoors, often during hours of peak sun intensity, represent a chronic, high-intensity assault of UVB radiation on the unprotected skin of the face. This cumulative exposure dramatically increases the probability of critical, cancer-initiating mutations occurring within the epidermal stem cells of the periorbital region, thus providing the definitive trigger for the entire carcinogenic process (Figure 6). The second stage of the figure transitions from the external environment to the internal, molecular machinery of the cell, detailing the specific consequences of the UV-induced DNA damage (Figure 6). The flowchart clearly illustrates that the damage leads to a loss-of-function mutation in a critical tumor suppressor gene known as PTCH1. This gene is the gatekeeper of the Hedgehog signaling pathway, a cellular communication network that is essential for embryonic development but is normally suppressed in most adult tissues, including the skin.[19] In its normal, unmutated state, the PTCH1 protein acts as a receptor that tonically inhibits another protein called Smoothened (SMO). It functions as the "brakes" on the pathway. The figure shows that when UV radiation causes a loss-of-function mutation in PTCH1, these brakes are effectively cut. The mutated PTCH1 protein can no longer restrain SMO, leading to its spontaneous and unregulated activation. The activation of SMO is the key initiating event in the molecular cascade. The now-active SMO protein sends a signal into the cell that ultimately activates a family of transcription factors known as GLI. Transcription factors are proteins that can enter the cell's nucleus, bind to specific regions of the DNA, and turn on the expression of specific genes.[19] The activated GLI proteins, as shown in the figure, are the final messengers that execute the pathway's command: they switch on a suite of genes responsible for promoting relentless cell division and survival. The result of this aberrant, unchecked signaling is cell proliferation. A single epidermal stem cell, now armed with a mutated PTCH1 gene, begins to divide uncontrollably, ignoring the normal signals that would tell it to stop. This marks the transformation from a normal cell into a malignant one, initiating the growth of the tumor. The final stage of the figure brilliantly connects the abstract concept of uncontrolled cell proliferation to the tangible, observable evidence seen in the patient (Figure 6). This section explains how the microscopic molecular events translate into the macroscopic and microscopic features that a clinician and pathologist can identify. First, the clinical finding is addressed. The relentless proliferation of millions of basaloid cells, driven by the hyperactive Hedgehog pathway, forms a physical mass within the skin. This growing nodule pushes up the overlying epidermis, creating a smooth, often translucent or "pearly" papule or plaque. As the tumor continues to enlarge, its central portion can outgrow its blood supply, leading to necrosis and the formation of a central ulcer.[20] This perfectly matches the clinical description of the patient's lesion as a pearly, ulcerated plaque on the eyelid, providing a direct physical manifestation of the underlying molecular process (Figure 6). Second,

the dermoscopic finding is explained. A growing tumor has high metabolic demands and requires a dedicated blood supply for oxygen and nutrients. To achieve this, it secretes growth factors that stimulate the formation of new blood vessels, a process called angiogenesis. These newly formed vessels are typically disorganized, dilated, and follow a chaotic, branching pattern. When viewed under the magnification of a dermatoscope, these vessels are visible as the classic arborizing vessels—large, tree-like red lines that are a hallmark of BCC. Therefore, the dermoscopic finding is a direct visual indicator of the tumor's neovasculature, a necessary support system for the uncontrolled cell proliferation (Figure 6). Finally, the Histopathological Finding provides the ultimate microscopic proof of the disease process (Figure 6). When the excised tissue is examined under a microscope, the sheets of proliferating cancer cells are seen as nodular aggregates of basaloid cells invading the dermis. The term "basaloid" refers to their resemblance to the basal cells of the epidermis, the origin of the cancer. A unique and diagnostic feature of these aggregates is peripheral palisading, where the nuclei of the cells at the very edge of each nest align themselves in a neat, fence-like row.[20] This highly organized arrangement at the tumor's periphery is a classic and reliable feature that allows the pathologist to confirm the diagnosis with a high degree of certainty. In essence, the histopathology slide provides a direct, magnified view of the "Cell Proliferation" that was initiated by the molecular cascade, completing the diagnostic circle.

## 4. Conclusion

This case report provides a methodologically detailed and scientifically grounded illustration of the successful use of a rhomboid flap for the reconstruction of a moderate-sized lower eyelid defect following the excision of a basal cell carcinoma. By adhering to sound oncologic principles, leveraging a deep understanding of molecular pathophysiology for diagnosis, and applying sophisticated biomechanical principles to the reconstructive design, a result was achieved that was successful by every objective measure: complete tumor clearance, preservation of normal eyelid function with the critical prevention of ectropion, and a cosmetically superior scar that led to high patient satisfaction. While the evidence from a single case must be interpreted with appropriate caution, this report strongly supports the rhomboid flap as a robust, reliable, and elegant option in the reconstructive surgeon's toolkit. It powerfully affirms that the ultimate goal of modern dermatologic surgery is not merely to cure a disease, but to restore the patient's form, function, and quality of life to the highest possible standard.

## 5. References


1. Swer D, Mahawar R, Sobita Devi Y, Sangtam D. Non-Hodgkins lymphoma of bilateral eyelids with basal cell carcinoma of nose: a rare case report. Int J Res Med Sci. 2024; 12(7): 2660–3.
2. Told R, Reumueller A, Kreminger J, Lackner B, Kuchar A, Schmidt-Erfurth U, et al. Long-term results after surgical basal cell carcinoma excision in the eyelid region: revisited. Wien Klin Wochenschr. 2025; 137(1–2): 7–12.
3. Lee K-I, Choi Y-W, Han S-K, Namgoong S, Jeong S-H, Dhong E-S. The potential of artificial dermis grafting following basal cell carcinoma removal on the lower eyelid. J Plast Reconstr Aesthet Surg. 2025; 100: 205–7.
4. Vass A, Polgár N, Sándor SA, Ágoston D, Rózsa P, Csányi I, et al. The role of electrochemotherapy in the treatment of locally advanced or recurrent eyelid-periocular basal cell carcinoma: long-term results. Int J Dermatol. 2025; 64(1): 111–8.
5. Huang Y, He C, Hu Q, Liu Z, Li X, Gao W, et al. Metabolic atlas of human eyelid infiltrative basal cell carcinoma. Invest Ophthalmol Vis Sci. 2025; 66(1): 11.
6. Mariños AP, Valverde-López J, Cárdenas Cruz P. Superficial basal cell carcinoma masquerading as pruritic dermatitis on the

upper eyelid. Acta Dermatovenerol Alp Panonica Adriat. 2025; 34(1): 41–3.
7. Bhandari AJ, Shirude AC, Jena A. Shades of concern-pigmented basal cell carcinoma of the eyelid. J Clin Ophthalmol Res. 2025; 13(2): 227–9.
8. Yazıcı B, Gonen T. Basal cell carcinoma kissing with nodular nevus on the eyelid margin: a causality or coincidence? Orbit. 2025; 44(4): 439–42.
9. Anastasopoulos I, Ntamagkas A, Chrysikos D, Patelis A, Troupis T. Basal cell carcinoma of the right lower eyelid treated with tarsoconjunctival and Mustardé flaps. Cureus. 2025; 17(2): e79129.
10. Jain A, Saini N, Yamini Y, Gole G. Mustarde's flap for post basal cell carcinoma excision lower eyelid reconstruction: Our experience. J Evid Based Med Healthc. 2015; 2(26): 3924–8.
11. Rodriguez-Garijo N, Redondo P. Linear basal cell carcinoma of the lower eyelid: Reconstruction with a musculocutaneous transposition flap. JAAD Case Rep. 2018; 4(7): 633–5.
12. Oley MH, Oley MC, Gunawan DF, Rangan AA, Wagiu AMJ, Faruk M. Adjunctive hyperbaric oxygen therapy with reconstruction of lower eyelid for basal cell carcinoma: a case series. Int J Surg Case Rep. 2023; 103(107890): 107890.
13. Bejinariu CG, Popescu S, Dragosloveanu CDM, Marinescu SA. Reconstruction of lower eyelid defects after the excision of basal cell carcinoma. Rom J Ophthalmol. 2020; 64(4): 414–8.
14. Redondo P, Barrio J, Salido-Vallejo R, Tomás-Velázquez A. Simplified lower eyelid reconstruction algorithm after basal cell carcinoma surgery: a retrospective series of patients. J Eur Acad Dermatol Venereol. 2023; 37(4): e496–8.
15. Baruah P, Bhuyan J, Boro M. Modified island pedicle advancement cheek flap for optimal reconstruction of cutaneous defects after excisional biopsy of basal cell carcinoma right lower eyelid. Indian J Ophthalmol Case Rep. 2023; 3(3): 793–4.
16. Mitra S, Panda S, Singh CA, Thakar A. Modified Mustardé flap for lower eyelid reconstruction in basal cell carcinoma: Revisited. Indian J Otolaryngol Head Neck Surg. 2023; 75(3): 2492–5.
17. Chietra YAM, Hatibie MJ, Dali R. Reconstruction of lower eyelid in basal cell carcinoma case with adjunctive hyperbaric oxygen therapy: a case report. Med Scope J. 2024; 7(1): 34–8.
18. Perri F, Di Monta G, D'Antonio S, Perrella PP, De Rosa A, Rullo V, et al. Reconstruction of full-thickness lower eyelid defects after basal cell carcinoma excision using a modified Hughes procedure. Plast Reconstr Surg Glob Open. 2025; 13(5): e6600.
19. Turcu EG, Ciuc D. Combined facial reconstruction for basal cell carcinoma involving the left nasal Ala and lower eyelid: Case presentation and surgical approach. Universal Library of Medical and Health Sciences. 2025; 03(02): 47–53.
20. Ikoma T, Amagata Y, Fujii K, Aoki M, Tozawa T, Iwata M, et al. Outcomes of free tarsoconjunctival grafts in lower eyelid reconstruction following basal cell carcinoma surgery. J Dermatol. 2025; (1346-8138.17872).